Available online at www.sciencedirect.com
SCIENCE DIRECT®
Journal of Molecular Catalysis A: Chemical 212 (2004) 323–328
JOURNAL OF MOLECULAR CATALYSIS A: CHEMICAL
www.elsevier.com/locate/molcata

Photocatalytic property of sillenite $Bi_{24}AlO_{39}$ crystals

W.F. Yao [a,*], X.H. Xu [a], J.T. Zhou [a], X.N. Yang [a], Y. Zhang [a], S.X. Shang [b], H. Wang [a], B.B. Huang [a]

[a] *State Key Lab of Crystal Materials, Shandong University, Jinan 250100, PR China*
[b] *Department of Environment Engineering, Shandong University, Jinan 250100, PR China*

Received 28 June 2003; received in revised form 16 November 2003; accepted 17 November 2003

Abstract

$Bi_{24}AlO_{39}$ crystals with sillenite structures were prepared by the chemical solution decomposition (CSD) method. The prepared powders were examined by the XRD and UV-Vis reflectance spectroscopy. The band gap of $Bi_{24}AlO_{39}$ crystals was estimated to be about 2.46 eV from the UV-Vis diffuse reflectance spectrum of the photocatalyst. Photocatalytic properties of $Bi_{24}AlO_{39}$ catalysts were evaluated using methyl orange as a model organic compound. The photocatalytic activity of the prepared $Bi_{24}AlO_{39}$ is high enough to photo-degrade 20 mg/l methyl orange in 2 h, which is similar as that of P-25 and much better than that of anatase TiO_2 prepared by us.
© 2003 Elsevier B.V. All rights reserved.

Keywords: Bi-O polyhedra; Chemical solution decomposition; Photo-degrade

1. Introduction

Recently photocatalysis, using semiconductors, such as TiO_2, has attracted extensive attention, because they provide a promising strategy for cleaning polluted air or water [1]. Previous studies have shown that such semiconductors can degrade most kinds of persistent organic pollutant, such as dyes, pesticide, detergents and volatile organic compounds, under UV-light irradiation [1–4]. However, the fast recombination rate of photogenerated electron/hole pairs hider the commercialization of this technology [1,2]. It is, therefore, of interest to develop new photocatalysts with higher photocatalytic properties. In an earlier study one of the author reported sillenite $Bi_{12}TiO_{20}$ as a novel photocatalyst against methyl orange [5,6]. The higher activity of sillenite $Bi_{12}TiO_{20}$ photocatalyst than that of anatase TiO_2 is attributed to the Bi-O polyhedra in $Bi_{12}TiO_{20}$ crystals, which were assumed to eliminate the recombination of electron–hole pairs and then facilitate the photocatalytic activity of the catalysts [5]. Because all sillenite crystals have the Bi-O polyhedra similar as those of $Bi_{12}TiO_{20}$, it is of great interest to examine other sillenite crystals. In the present paper, another sillenite photocatalyst $Bi_{24}AlO_{39}$ was reported. $Bi_{24}AlO_{39}$ crystals belong to a family of sillenite compounds with the general formula $Bi_{12}MO_{20}$ where M represents a tetravalent ion or a combination of ions. The overall structure of the $Bi_{12}MO_{20}$ crystal may be described in terms of the 7-oxygen coordinated Bi polyhedra, which share corners with other identical Bi polyhedra and with MO_4 tetrahedra. This body centered cubic structure of sillenite crystals facilitate the solubility of novel metal ions in the crystals, because the tetrahedron of oxygen atoms surrounding the M atoms is able to expand or contract without a major effect on the remaining atomic arrangement [7]. $Bi_{24}AlO_{39}$ is in sillenite $Bi_{12}MO_{20}$ type with 26 metal atoms per cell.

In this paper the sillenite $Bi_{24}AlO_{39}$ was synthesized by the chemical solution decomposition (CSD) method and photocatalytic properties of $Bi_{24}AlO_{39}$ catalysts were evaluated using methyl orange as a model organic compound.

2. Experimental

The sillenite crystals of $Bi_{24}AlO_{39}$ were prepared by the chemical solution decomposition (CSD) method with high purity grade chemicals of bismuth nitrate ($Bi(NO_3)_3{\cdot}5H_2O$) and aluminum nitrate ($Al(NO_3)_3{\cdot}9H_2O$). Glacial acid (CH_3COOH) was selected as a solvent. Bismuth nitrate ($Bi(NO_3)_3{\cdot}5H_2O$) and aluminum nitrate ($Al(NO_3)_3{\cdot}9H_2O$)

* Corresponding author. Tel.: +86-531-8564204; fax: +86-531-8565403.
E-mail address: weifengyao@icm.sdu.edu.cn (W.F. Yao).

1381-1169/$ – see front matter © 2003 Elsevier B.V. All rights reserved.
doi:10.1016/j.molcata.2003.11.012

were dissolved in glacial acetic acid (CH_3COOH), The solution was diluted with 2-methoxyethanol (CH_3OCH_2OH) to adjust the viscosity and surface tension of the solution. After being stirred for 2 h by a magnetic stirrer, the solution was dried at 100 °C for tens of minutes to remove the solvents and some organic materials. The obtained powders were then calcined at 600 °C for 5–30 min to produce crystallinity.

X-ray diffraction (XRD) measurement was carried out at a room temperature by using a Rigaku D/MAX-YA X-ray diffractometer with Cu-Kα radiation. The accelerating voltage of 40 kV, emission current of 20 mA and the scanning speed of $10^\circ\ m^{-1}$ were used. To determine the band gap energy of the photocatalysts, UV-Vis reflectance spectroscopy measurement was carried out using a Hitachi U-3000 spectrophotometer with an integrating sphere. The pure powdered $BaSO_4$ was used as a reference sample.

The photodecolorization of aqueous methyl orange was carried out in a 150 ml Pyrex glass vessel with constant magnetic stirring. A 20 W UV lamp with a maximum emission at about 360 nm was used as the light source. Reaction suspension was prepared by adding the prepared samples into a 50 ml of aqueous methyl orange solution. In all experiments, prior to irradiation, the suspensions were ultrasonically sonicated for 10 min and then magnetically stirred in a dark condition for 10 min to establish adsorption/desorption equilibrium. The suspensions were then irradiated under the UV light. The distance between the liquid surface and the light source was about 5 cm, where the light intensity was about 0.936 mW/cm^2 measured by using an UV-Vis spectrophotometer. The concentrations of aqueous methyl orange were determined by measuring the absorbance at 464 nm with an UV-Vis spectrophotometer.

3. Results and discussions

3.1. Characterization of the prepared samples

Fig. 1 shows the XRD patterns of $Bi_{24}AlO_{39}$ crystals calcined at a fixed temperature at 600 °C for 5, 10 and 30 min, respectively. As shown in Fig. 1, the prepared samples have

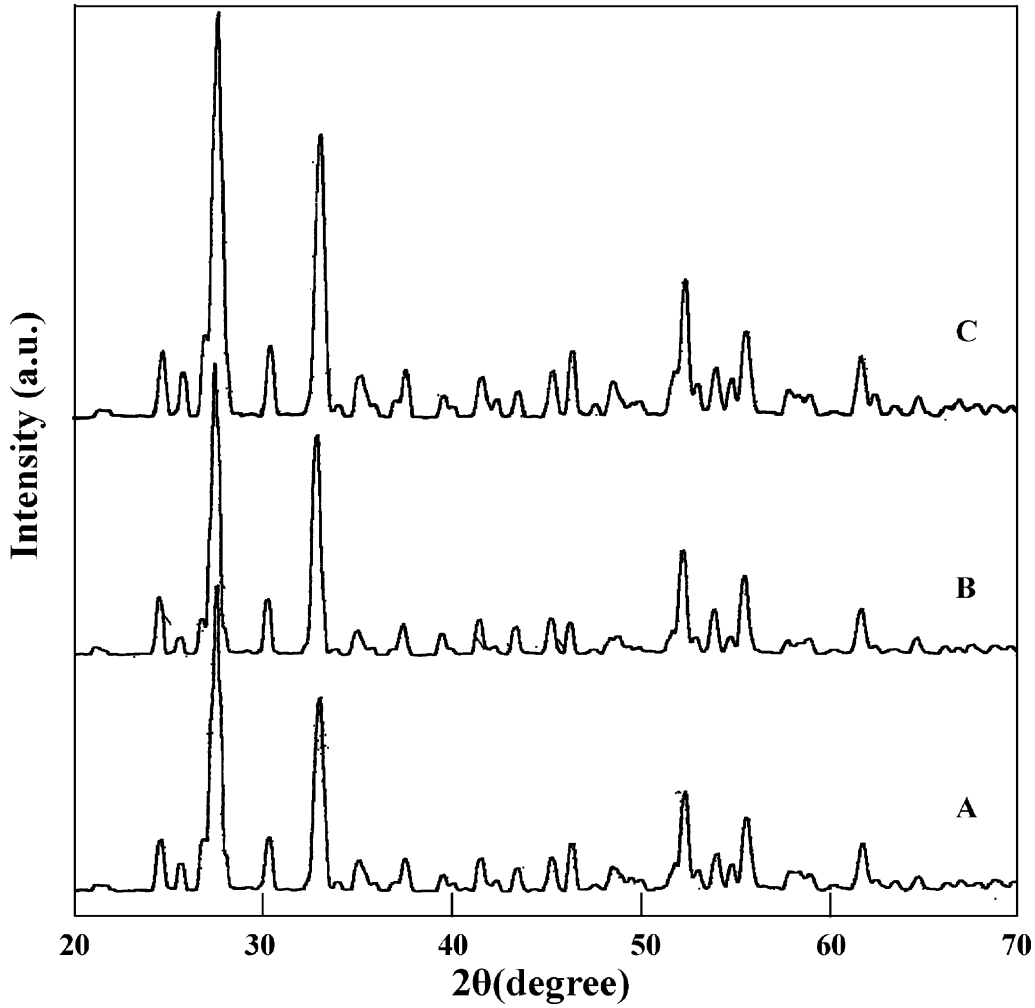

Fig. 1. X-ray diffraction patterns of as-prepared $Bi_{24}AlO_{39}$ powders calcined at a fixed temperature at 600 °C for 5, 10 and 30 min, respectively: (A) 5 min; (B) 10 min; (C) 30 min.

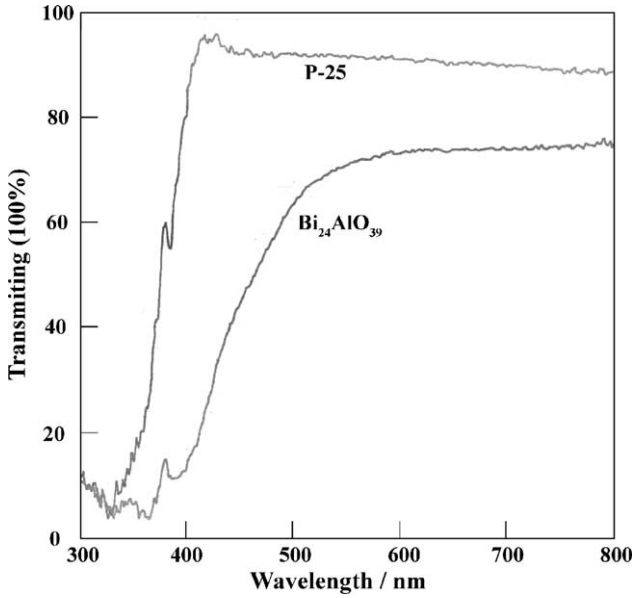

Fig. 2. The UV-Vis diffuse reflectance spectrum of $Bi_{24}AlO_{39}$ and P-25.

been well-crystallized at an annealing temperature of 600 °C for 5 min. The X-ray diffraction patterns of which were indexed based on the cubic lattice ($a = b = c = 10.179$ Å) as reported previously. According to Joint Committee of Powder Diffraction Standard data cards (42–184), most of the peaks emerged belong to $Bi_{24}AlO_{39}$ phase. This means that $Bi_{24}AlO_{39}$ can be prepared when calcined at 600 °C for 5 min. The XRD peaks of $Bi_{12}TiO_{20}$ become sharper and the full width at half maximum decreased, as shown in Fig. 1, indicating a better crystallinity and an increase in grain size when sintered at higher temperature.

The UV-Vis diffuse reflectance spectrum of $Bi_{24}AlO_{39}$ is as shown in Fig. 2. For comparison, the UV-Vis diffuse reflectance spectrum of P-25 is also presented. The band gap absorption edge of $Bi_{24}AlO_{39}$ and P-25 are determined to be 506 and 388 nm, corresponding to the band gap energy of 2.46 and 3.2 eV, respectively. For $Bi_{24}AlO_{39}$ with the band gap energy of 2.46 eV, theoretically it can be exited by the photons with the wavelength under 519 nm. While it is known that the methyl orange solution has a strong absorption at 400–500 nm, which is the main part of the visible light absorption of $Bi_{24}AlO_{39}$, so the methyl orange solution is not suitable to examine the photocatalytic activity of $Bi_{24}AlO_{39}$ under the irradiation of visible light. In this paper, we just examined the photocatalytic activity of $Bi_{24}AlO_{39}$ under the irradiation of UV-light.

3.2. Photocatalytic activity of $Bi_{24}AlO_{39}$ crystals

The UV-Vis spectra for methyl orange solution show two absorption maxima, the first band observed at 270 nm and the second band at 464 nm. The band at 464 nm was used to monitor the effect of the photocatalysis on the degradation of methyl orange. It is known that methyl orange can be adsorbed onto catalysts from its aqueous solution. Hachem et al. [8] pointed out that the absorption was quite fast and the equilibrium concentration could be reached within about 45 min. In this paper, the absorption/desorption equilibrium of the suspensions was established by ultrasonically sonicated for 10 min and then magnetically stirred in a dark condition for 10 min. The photocatalytic degradation generally follows a Langmuir–Hinshelwood mechanism [9,10], with the rate r being proportional to the coverage θ which becomes proportional to C at low concentrations

$$r = k\theta = \frac{k\mathrm{KC}}{1 + \mathrm{KC}} \tag{1}$$

where k if the true rate constant and K the adsorption constant. Since the initial concentration is low ($C_0 = 20$ mg/l), the term KC in the denominator can be neglected and the rate becomes, apparently, first order

$$r = -\frac{\mathrm{d}c}{\mathrm{d}t} = k\mathrm{KC} = k_{\mathrm{app}}C \tag{2}$$

where k_{app} is the apparent rate constant of pseudo-first order. The integral form $c = f(t)$ of the rate equation is

$$\ln\frac{C_0}{C} = k_{\mathrm{app}}t \tag{3}$$

3.3. Effect of catalysts concentration on the photocatalytic activity

In order to determine the optimal amount of photocatalyst, a preliminary study (Fig. 3) has been carried out to optimize the concentration of $Bi_{24}AlO_{39}$ catalysts. The amount of the photocatalyst was varied from 2 to 7 g/l. The concentration of methyl orange decreased negligibly over the time span of these experiments in the absence of photocatalysts. A blank experiment in the absence of irradiation but with the prepared catalysts demonstrates that no significant change in the concentration was found. As shown in Fig. 3, the photocatalytic activity of $Bi_{24}AlO_{39}$ has significant difference

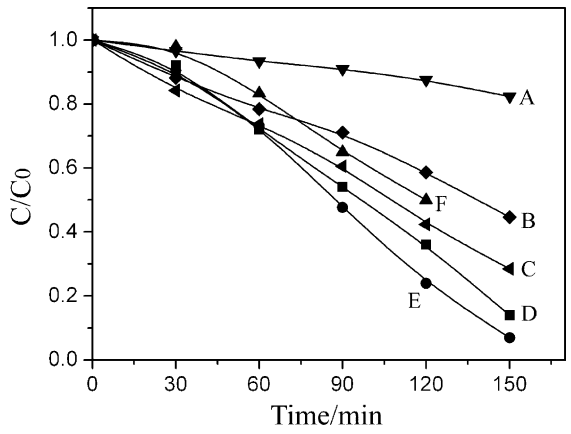

Fig. 3. The decreases of methyl orange solution by different concentration of $Bi_{24}AlO_{39}$ crystal as a function of UV irradiation time. The concentrations of the catalyst are: (A) 2 g/l; (B) 3 g/l; (C) 4 g/l; (D) 5 g/l; (E) 6 g/l; (F) 7 g/l, respectively.

Table 1
Summary of the apparent reaction rate constants calculated from Figs. 3 and 4 for different catalysts

Catalysts	Annealing times (min)	Catalyst concentration (g/l)	Apparent reaction rate constants ($k \times 10^{-3}$ min^{-1})	Methyl orange decolorization (min)[a]
$Bi_{24}AlO_{39}$	5	6	9.1	76.2
$Bi_{24}AlO_{39}$	10	6	16	43.3
$Bi_{24}AlO_{39}$	30	2	1.3	533
$Bi_{24}AlO_{39}$	30	3	4.6	150.7
$Bi_{24}AlO_{39}$	30	4	8.2	84.5
$Bi_{24}AlO_{39}$	30	5	10.5	66
$Bi_{24}AlO_{39}$	30	6	12.2	56.8
$Bi_{24}AlO_{39}$	30	7	7.8	88.9
P-25	–	2	16.8	41.3
Anatase TiO_2[b]	–	3	4.95	140

[a] Time required for 50% decolorization of 20 mg/l methyl orange solution.
[b] Pure anatase TiO_2 nanopowders prepared by us.

among the photocatalysts concentrations varied from 2 to 7 g/l. The calculated apparent reaction rate constants of each catalyst are listed in Table 1. The experiment results appear that the degree of decolorization of dye solution increases with increasing amount of photocatalyst, reaches the higher value at catalyst loading = 6 g/l and then decreases. Similar phenomena were found in the study of the photocatalyst of P-25, which reached the higher value at catalyst loading = 2 g/l [11]. This behavior is attributed to the so-called shielding effect after exceeding the optimal amount, the suspended catalysts reduces the penetration of the light in the solution [12]. Because the most active was the photocatalyst with concentration of 6 g/l, the rest of experiments were carried out using this concentration.

3.4. Effect of heat-treatment for photocatalyst on the photocatalytic activity

The effect of heat-treating times on the photocatalytic activity of $Bi_{24}AlO_{39}$ at a fixed temperature of 600 °C is examined (Fig. 4). It can be seen that the degradation rate of methyl orange increases with the increasing annealing times. As shown in Fig. 4 and Table 1, the sample calcined at 600 °C for 10 min displays photocatalytic activity with a constant of 0.016 min^{-1}, which is much better than that of pure anatase TiO_2 prepared by us. As a comparison, P-25 and the pure TiO_2 prepared by us need 2 and 3 h, respectively, to photodecolorize the 20 mg/l methyl orange solution under similar conditions. Yet further increase of the calcination times decreases the photocatalytic activity of the prepared sample, when the calcination times reach to 30 min the prepared sample shows a lower rate constant of 0.012 min^{-1}. The enhancement of photocatalytic activity at the increasing calcinations time from 5 to 10 min can be attributed to an obvious improvement in the crystallinity of $Bi_{24}AlO_{39}$ (as shown in Fig. 1). While long calcinations time will cause the dramatically growth of particle, leading to the decrease in BET, therefore, resulting in the decrease in the photocatalytic activity [2–14].

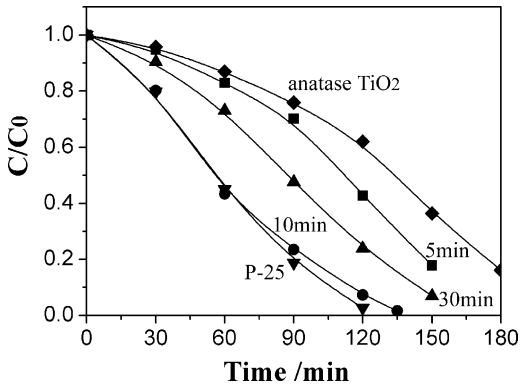

Fig. 4. The effect of heat-treating times on the photocatalytic activity of $Bi_{24}AlO_{39}$ at a fixed temperature of 600 °C. The catalysts are: $Bi_{24}AlO_{39}$ calcined for 5, 10, 30 min, P-25, and anatase TiO_2 prepared by us, respectively.

3.5. Effect of initial dye concentration on the photocatalytic activity

The effect of initial dye concentration in water on the photocatalytic process was examined. The reactions of dye decomposition were carried out in the range 5–20 mg/l. As shown in Fig. 5, the photocatalytic activity of $Bi_{24}AlO_{39}$ has no significant difference among the initial dye concentrations varied from 5 to 20 mg/l. It was found that the best degradation was obtained with 20 mg/l methyl orange. The result is different with that obtained for the degradation of methyl orange by using TiO_2 where the degradation rate decreases with increasing the initial dye concentration [15], which can be related to the formation of several layers of adsorbed dye on the photocatalyst surface and then inhibits the reaction of dye molecules with photogenerated holes or hydroxyl radicals. As to $Bi_{24}AlO_{39}$ catalysts, it seems that the initial dye concentration has little effect on the photocatalytic activity of the photocatalysts.

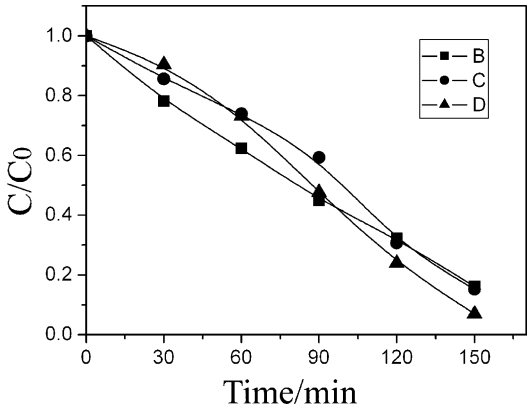

Fig. 5. The effect of initial dye concentration on the photocatalytic activity of $Bi_{24}AlO_{39}$: (B) 5; (C) 10; (D) 20 mg/l, respectively.

3.6. Effect of pH on the photocatalytic activity

The heterogeneous photocatalysis has been found to be pH dependent [2,15–18]. As shown in Fig. 6, the reaction rate increase at acidic pH but decrease at alkaline pH. It appears that the effect of pH on the degradation of the pollutions is variable and controversial. For example, bahnemann et al. [16] found the photocatalytic degradation rate of $CHCl_3$ at pH 8–9 is about 10 times higher than that at pH 3.8. In our case the highest degradation rate was achieved at pH = 2. Similar results were previously observed for the photodecomposition of 3-chlorophenol [17] and degradation of methyl orange [2,15], which was explained on the basis that at low pH HO_2 radicals will form, and this will compensate for the effect of decreasing hydroxyl ions concentration. The decrease in degradation rate at alkaline pH is assumed to the anions and the highly negative charged oxide surface and degradation would, thus, depend on diffusion of surface-generated OH towards the inside layer to the low concentration of methyl orange anion, a slower process than direct charge transfer [2,18].

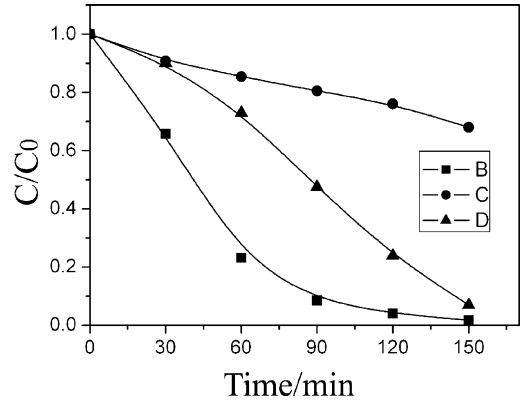

Fig. 6. The effect of pH on the photocatalytic activity: (B) pH = 2; (C) pH = 9; (D) pH = 7, respectively.

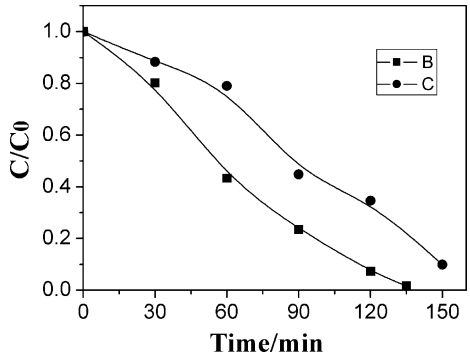

Fig. 7. The effect of methanol addition on the photocatalytic activity of $Bi_{24}AlO_{39}$: (B) no methanol addition; (C) 0.1 M methanol addition. [methyl orange] = 20 mg/l.

3.7. The mechanism of photocatalytic activity of methyl orange on $Bi_{24}AlO_{39}$

It has been shown that the photodegradation of dyes is closely related to the adsorption of dyes on the surface of the photocatalysts, and the degradation takes place at or near to the catalyst particle surface, rather than in the bulk solution [19,20]. For the $Bi_{24}AlO_{39}$ catalysts, as state previously, the absorption/desorption equilibrium of the suspensions was established before the UV light irradiations. To examine the surface reaction mechanism, methanol was added to the dispersion. This alcohol has been found to both scavenge holes and react with $OH^{\bullet}$ [21,22]. As shown in Fig. 7, the 0.1 M methanol addition shows drastic inhibitive effect on the photodegradation of methyl orange. Since methanol did not strongly adsorb on $Bi_{24}AlO_{39}$ in aqueous systems and compete for sites, the decrease of the activity of $Bi_{24}AlO_{39}$ can be attributed to the competitive of the holes or $OH^{\bullet}$ between the methyl orange and the methanol in the diluted solutions. The results suggest that the degradation of the methyl orange can be partly taken place in the bulk solution.

The origin of the higher photocatalytic activity of $Bi_{24}AlO_{39}$ crystals is of great interest. In the study of photocatalytic properties of sillenite $Bi_{12}TiO_{20}$, the high activity of sillenite $Bi_{12}TiO_{20}$ photocatalyst is attributed to the Bi-O polyhedra in the sillenite crystal structure [5]. In this paper we proposed that the sillenite structure of $Bi_{24}AlO_{39}$ crystals can also be regarded as one important factor to affect the photocatalytic property of the crystals. The process of photodecomposition of organic pollution on solid catalysts is always depicted as resulting from continuous band-gap irradiation of the aqueous semiconductor dispersion that excites an electron from the valence band to the conduction band, creating an electron–hole pair. Photo-generated holes are capable of directly oxidizing many organic pollutants, and photogenerated electrons have also been shown to be capable of contributing to the decomposition process through reduction of absorbed O_2 to the superoxide radical ion, $O_2^{-\bullet}$ [14,23]. It is important to separate the

photo-generated holes and electrons pairs to improve the photocatalytic activity of the catalyst. Recently, Gerischer and Heller [24] found that the rate of photooxidation is equal to and limited by the reduction rate of dissolved oxygen (O_2) in the solution. It was theoretically predicted that, when O_2 is not reduced at a sufficiently high rate, electrons will accumulate on the photocatalyst particles and the electron–hole recombination will be enhanced [3,24]. Recently researchers found that some oxides, such as Bi_2O_3, play a role of active oxygen donors in photo-oxidation process [25]. Tsubo et al. [26] showed that gaseous oxygen become active only after passing through the volume of a grain of such donor oxides. Bi-O polyhedra in $Bi_{24}AlO_{39}$ crystals were assumed to serve as the active donor sites, which can enhance the electron transfer to O_2 and eliminate the recombination of electron–hole pairs. The origin of the high photocatalytic property of $Bi_{24}AlO_{39}$ crystals need further study.

4. Conclusions

$Bi_{24}AlO_{39}$ crystals with sillenite structures were prepared by the chemical solution decomposition (CSD) method. The band gap of $Bi_{24}AlO_{39}$ crystals was estimated to be about 2.46 eV from the UV-Vis diffuse reflectance spectrum of the photocatalyst. The photocatalyst based on $Bi_{24}AlO_{39}$ crystals for photo-decolorization of methyl orange has been examined. The high photocatalystic activity of the prepared sample is supposed to be facilitated by the Bi-O polyhedra of $Bi_{24}AlO_{39}$ crystals.

Acknowledgements

This work was supported by the National 863 High Tech Program of China, Shandong science and technology Foundation and Shandong University.

References

[1] M.R. Hoffmann, S.T. Martin, W.Y. Choi, D.W. Bahnemann, Chem. Rev. 95 (1995) 69.
[2] C. Wang, J. Zhao, X. Wang, B. Mai, G.S. heng, P. Peng, J. Fu, Appl. Catal. B: Environ. 39 (2002) 269.
[3] A.L. Linsebigler, G.Q. Lu, J.T. Yates Jr., Chem. Rev. 95 (1995) 735.
[4] T. Torimoto, S. Ito, S. Kuwabata, H. Yoneyama, Environ. Sci. Technol. 30 (1996) 1275.
[5] W.F. Yao, H. Wang, X.H. Xu, X.F. Cheng, J. Huang, S.X. Shang, X.N. Yang, M. Wang, Appl. Catal. A: Gen. 243 (2003) 185.
[6] W.F. Yao, H. Wang, X.H. Xu, J.T. Zhou, X.N. Yang, Y. Zhang, S.X. Shang, M. Wang, Chem. Phys. Lett. 377 (5–6) (2003) 501–506.
[7] S.C. Abrahams, J.L. Bernstein, C. Svensson, J. Chem. Phys. 71 (2) (1979) 788.
[8] C. Hachem, F. Bocquillon, O. Zahraa, M. Bouchy, Dyes Pigments 49 (2001) 117–125.
[9] A. Houas, H. Lachheb, M. Ksibi, E. Elaloui, C. Guillard, J.-M. Hertmann, Appl. Catal. B: Environ. 31 (2001) 134.
[10] J.C. Yu, J. Yu, J. Zhao, Appl. Catal. B: Environ. 36 (2002) 31.
[11] A. Rachel, M. Sarakha, M. Subrahmanyam, P. Boule, Appl. Catal. B: Environ. 37 (2002) 293.
[12] J. Grzechulska, A.W. Morawski, Appl. Catal. B: Environ. 36 (2002) 45.
[13] L.G. Devi, G.M. Krishnaiah, J. Photochem. Photobiol. Part A: Chem. 121 (1999) 141.
[14] A.S. James, C. Cristian, C. Adriana, Chem. Rev. 95 (1995) 477–510.
[15] A.-Q. Siham, R.S. Salman, J. Photochem. Photobiol. Part A: Chem. 148 (2002) 161.
[16] D. Bahnemann, D. Bockelmann, R. Goslich, Solar Energy Mater. 24 (1991) 564.
[17] K. Young, C.-B. Hsich, Water Res. 26 (11) (1992) 1451.
[18] I. Poulios, M. Kositzi, A. Kouras, J. Photochem. Photobiol. Part A: Chem. 115 (1998) 175.
[19] C. Hu, Y. Wang, H. Tang, Appl. Catal. Environ. 30 (2001) 277.
[20] G. Liu, X. Li, J. Zhao, H. Hidaka, N. Serpone, Environ. Sci. Technol. 34 (2000) 3982.
[21] M. Uimann, J. Augustynky, Chem. Phys. Lett. 141 (1987) 154.
[22] R. Matthews, J. Chem. Soc., Faraday Trans. 180 (1984) 457.
[23] Y.A. Cao, X.T. Zhang, W.S.H. Yang, H. Du, Y.B. Bai, T.J. Li, J.N. Yao, Chem. Mater. 12 (2000) 3445–3448.
[24] H. Gerischer, A. Heller, J. Electrochem. Soc. 139 (1992) 113.
[25] L. Weng, B. Delmon, Appl. Catal. A 81 (1992) 141.
[26] T. Tsubo, H. Hiura, Y. Horikawa, T. Shirasaki, J. Catal. 36 (1975) 240.